

See discussions, stats, and author profiles for this publication at:  
<https://www.researchgate.net/publication/251465417>

# Chapter 12 Theoretical design of electronically stabilized molecules containing planar tetracoordinate carbons

ARTICLE · JANUARY 2007

DOI: 10.1016/S1380-7323(07)80013-6

---

READS

16

3 AUTHORS, INCLUDING:



Alberto Vela

Center for Research and Advanc...

126 PUBLICATIONS 2,519 CITATIONS

SEE PROFILE



Miguel A Méndez-Rojas

Universidad de las Américas Pue...

65 PUBLICATIONS 720 CITATIONS

SEE PROFILE

## Chapter 12

# Theoretical design of electronically stabilized molecules containing planar tetracoordinate carbons

<sup>a</sup>Alberto Vela, <sup>b</sup>Miguel A. Méndez-Rojas, and <sup>c</sup>Gabriel Merino

<sup>a</sup>Departamento de Química, Cinvestav, A. P. 14-740 México, D.F., 07000, México,

<sup>b</sup>Departamento de Química y Biología, Universidad de las Américas, Puebla, Ex-Hda. de Sta. Catarina Martir, Cholula 72820, Puebla, México and

<sup>c</sup>Facultad de Química, Universidad de Guanajuato. Col. Noria Alta s/n C.P. 36050, Guanajuato, Gto., México

### 1. Brief historical background

In the early days of chemistry, Edward Frankland suggested the idea of valence to explain the building of several organometallic compounds<sup>1</sup>. It was the first step toward understanding the structure of organic molecules. In 1856, Couper<sup>2</sup> and Kekule<sup>3</sup> came to the conclusion that carbon is tetravalent. Later, van't Hoff<sup>4</sup> and LeBel<sup>5</sup> established a relationship between optical activity and the atomic spatial arrangement. These proposals are milestones of organic chemistry. A tetrahedral molecule with a central carbon atom and four different ligands has two different arrangements in space which are mirror images of each other. Thus, this “simple” three-dimensional (3D) vision of molecular structure paved the way to the fundamental concept of chirality in chemistry. In 1848, Pasteur resolved the two optically active forms of tartaric acid, and a few years later he realized that the handedness of the carbon atom had a paramount importance in the biological activity of compounds. Nowadays, it is solidly established that the absolute configuration of molecules crucially determines its biological activity.

During the twentieth century, new molecular species with carbon atoms in unusual environments were proposed, opening what can be called the *inorganic side of carbon*. For example, carbon can be surrounded by more than four ligands.<sup>6</sup> The fascinating chemistry of hypercarbons is very nicely presented in Olah's Nobel lecture.<sup>7</sup> In 1970, almost a century after van't Hoff and LeBel tetrahedral model was published, Hoffmann, Alder, and Wilcox suggested an idea, challenging the structural foundations of organic

chemistry.<sup>8</sup> In their now classic paper, they presented a discussion, based on the molecular orbital structure of planar methane, about the electronic requirements necessary to stabilize a planar tetracoordinate carbon (ptC) atom. Inspired on this idea, several groups have successfully predicted, and even experimentally characterized, molecules containing a ptC.<sup>9–14</sup> It is not pretentious to say that these discoveries have opened a new age for carbon chemistry. In this chapter, we summarize our recent contributions in this fascinating quest to find new molecules containing ptCs and to provide a rationale of their stability.

## 2. How to confine a ptC into a molecule?

Two general strategies have been used to stabilize a ptC in a molecule: one of them is purely electronic and the other is a steric enforcement of the planar orientation of the bonds, the so-called mechanical approach. Let us start with the simplest molecule containing a tetracoordinate carbon atom, methane ( $\text{CH}_4$ ). If one forces it to acquire a planar  $D_{4h}$  structure, the central carbon atom adopts a  $sp^2$  hybridization, with one lone pair perpendicular to the molecular plane, the  $a_{2u}$  orbital depicted in Figure 1. By lowering the symmetry of  $\text{CH}_4$  from  $T_d$  to  $D_{4h}$ , only six electrons occupy bonding orbitals (orbitals  $e_u$  and  $a_{1g}$  in Figure 1), contrasting with the four bonding pairs present in  $T_d$  methane. The Hoffmann–Alder–Wilcox strategy to stabilize a ptC is to include the lone pair in the bonding framework by replacing one or more hydrogen atoms with good  $\sigma$ -donor/ $\pi$ -acceptor ligands, or by incorporating the lone pair into a  $(4n+2)\pi$  delocalized system.<sup>8</sup>

Several molecules containing a ptC were predicted, and even experimentally detected, using the electronic approach (Figure 2).<sup>15–21</sup> Among them, a beautiful series of pentaatomic molecules including a ptC were proposed by Boldyrev, Schleyer, and Simons and were experimentally detected by Wang and Boldyrev.<sup>22–28</sup> Interestingly, all these structures share a common feature—they have at least one atom, *different from carbon*, which is bonded to the ptC.

In the mechanical approach, geometrical constraints that force the central carbon atom and its nearest neighbors to be in a plane are imposed. The bonds can be constrained by rings and cages, as has been done in the family of molecules known as alkaphanes.<sup>13,29–34</sup> However, the experimental efforts done to isolate one of these mechanically stabilized molecules containing a ptC have been unfruitful. The lack of success may be due to the fact that the  $p$ -orbital normal to the ptC plane, generally the HOMO, is strongly

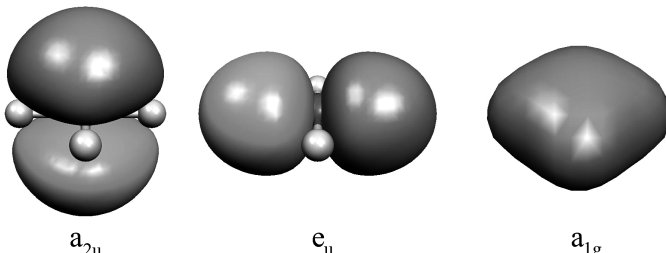


**Figure 1** Molecular orbitals of methane with  $D_{4h}$  symmetry

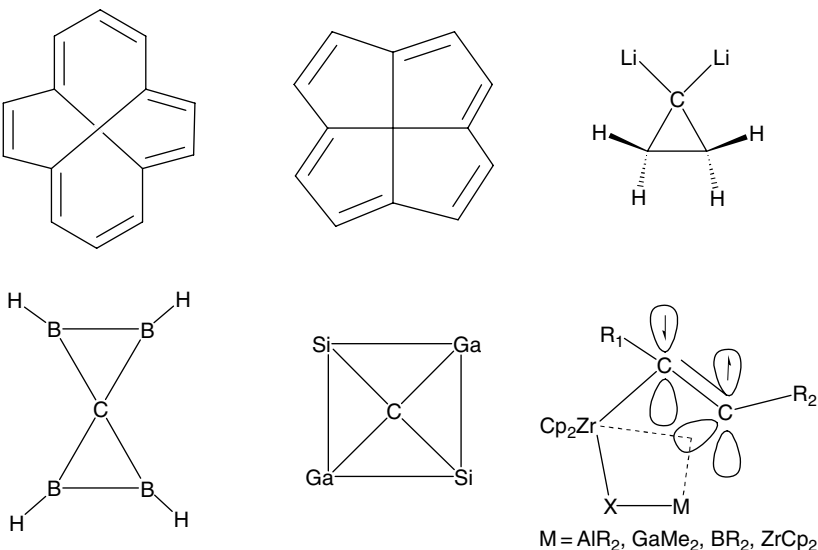


**Figure 2** Selected examples of molecules containing a ptC

localized on the central carbon atom, resulting in a cage that is held together by very weak forces that prevent its stabilization and, hence, its experimental isolation.

Despite all these *in vitro* and *in silico* efforts, the statement by Keese was still challenging the ptC's research community: "... no structures with a planar tetracoordinate C(C)<sub>4</sub> have been found..."<sup>35</sup> Two years later, Rasmussen and Radom<sup>30</sup> designed the first stable ptC surrounded only by carbons, [ptC(C)<sub>4</sub>], the dimethanospiro[2,2]octaplane (Figure 3).<sup>30</sup> Wang and Schleyer found a set of boron spiroalkanes with a ptC(C)<sub>4</sub> through substitution of carbon by boron atoms.<sup>36,37</sup> In 2003, a novel family of molecules based on a C<sub>5</sub><sup>2-</sup> moiety was proposed by us, which constituted the simplest and smaller set of molecules containing a ptC(C)<sub>4</sub>, and more importantly, the first and, at that time, the only one stabilized purely by electronic factors.<sup>38</sup>

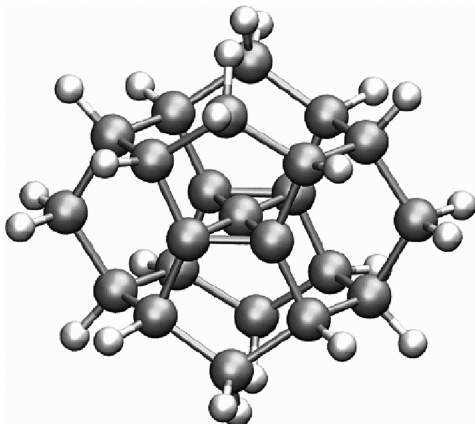
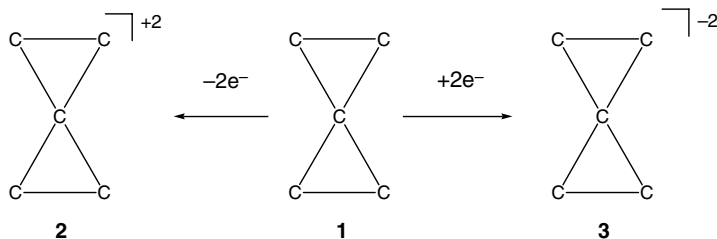


**Figure 3** Alkaplane proposed by Rasmussen and Radom<sup>30</sup>

## 2.1. $C_5^{2-}$ and $(C_5M_{2-n})^{n-}$

Obviously, the smallest possible cluster containing a  $C(C)_4$  skeleton is  $C_5$ . Experimental and theoretical studies showed that the global minimum of the neutral species is the linear structure, and there was no evidence of planar isomers of  $C_5$  containing a ptC.<sup>39,40</sup> We considered the possibility of extracting or adding electrons to this moiety and to search stable isomers on the potential energy surface (PES), aiming to find a  $C_5^n$  cluster containing a ptC.<sup>38,41</sup>



After removing two electrons one finds **2** as a stationary point with two imaginary frequencies. On the other hand, and to our pleasant surprise, the addition of two electrons to **1**, generates the local minimum **3** ( $C_5^{2-}$ ) having the desired ptC( $C_4$ ) atom. The  $D_{2h}$ -optimized geometry of  $C_5^{2-}$  is shown in Figure 4. Note that the largest C-C bond length (150.9 pm) is comparable with those calculated for dimethanospiro[2.2]octaplane (150.4 pm)<sup>14</sup> and several [4.4.4.5]fenestrene derivatives (149.3–152.9 pm).<sup>42</sup>

The experimental observation of  $C_5^{2-}$  strongly depends on the topography of the PES that drives the dynamics of the cluster and thus, its mean lifetime. To gain a better idea about the stability or metastability of the parental skeleton  $C_5^{2-}$ , an extensive exploration of its PES was performed (see Figure 5). Among all the stationary points located on the PES, only four were local minima, including **3**. Two of them (**1A** and **1B**) are lower in energy than **3** (202.4 and 184.8 kJ mol<sup>-1</sup>, respectively), whereas the 3D  $D_{3h}$  structure, **3C**, is 179.5 kJ mol<sup>-1</sup> higher in energy. Structure **1D** is the transition state involved in the rearrangement that isomerizes **1B** into **1**, and vice versa. It should be

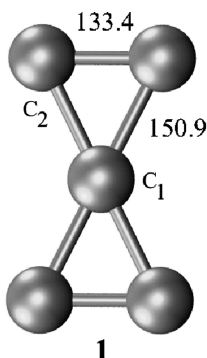


**Figure 4** B3LYP/6-311++G(2d)-optimized geometry of the parental skeleton  $C_5^{2-}$ .

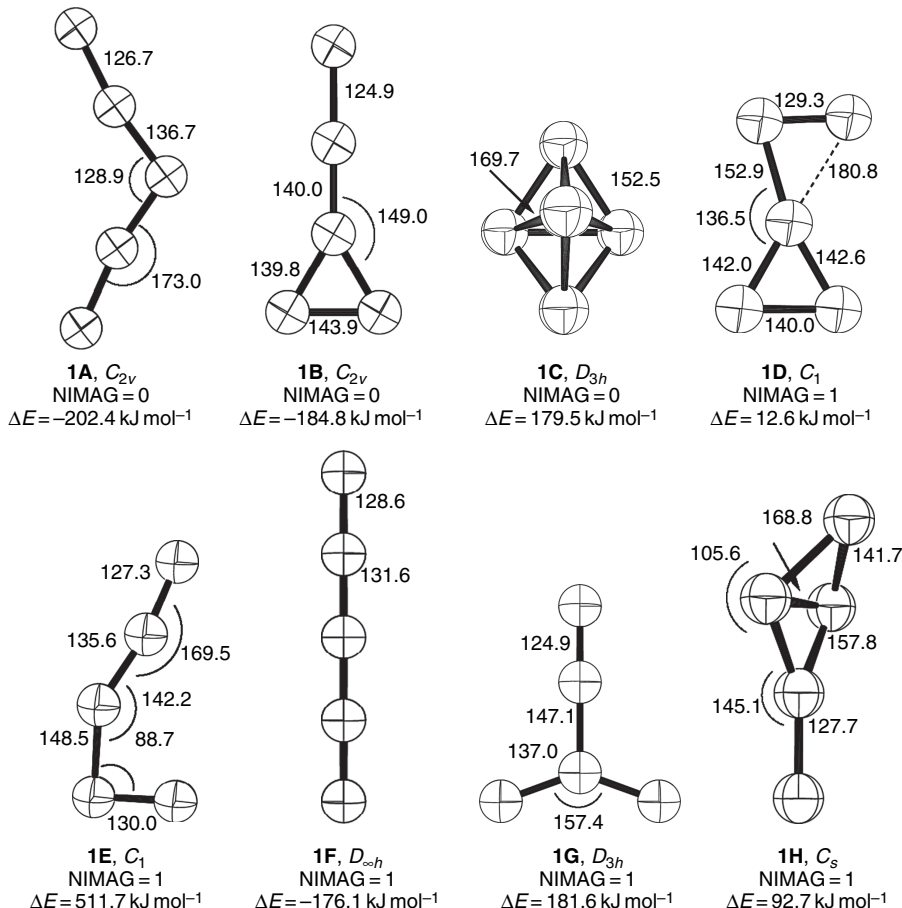


**Figure 5** Stationary points of the  $\text{C}_5^{2-}$  skeleton calculated with B3LYP/6-311++G(2d). NIMAG is the number of imaginary harmonic frequencies obtained for each structure using the same methodology, and  $\Delta E$  is the energy difference of the corresponding structure minus that of **3**, including the scaled ZPE (0.9806). All distances are in picometers and angles in degrees

noted that structure **1D** is not planar and lies very close in energy to **1** ( $12.6 \text{ kJ mol}^{-1}$ ). Structures **1E-1H** have one imaginary frequency, and they are not connected to the ptC-containing molecule. The MP2 and CCSD(T) calculations of the local minimum **3** confirm the stability of the dianion, supporting the results obtained with the hybrid exchange-correlation density functional.

Why  $\text{C}_5^{2-}$  is a local minimum? Consider a neutral spiropentadiene as a starting structure (Figure 6). After removing four protons from this latter compound,  $\text{C}_5^{4-}$  is obtained. This process generates four lone pairs, one on each terminal carbon and pointing outward, roughly in the direction where the hydrogen nuclei were located in the original structure. Now, after rotating one cyclopropenyl ring against the other, all five carbon atoms are in the same plane, and one ends up with the planar  $\text{C}_5^{4-}$ .

The central  $\pi$ -type lone pair, a characteristic feature of square planar carbon systems, will be surely destabilized. Vacating this MO will result in  $\text{C}_5^{2-}$  for which there are

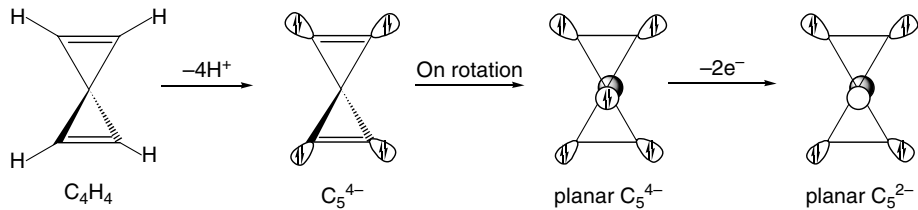


**Figure 6** Simplified picture of the construction of the MOs of  $\text{C}_5^{2-}$  from  $\text{C}_5^{4-}$  derived from  $\text{C}_5\text{H}_4$

four lone pairs pointing outward and a  $\pi$ -system of two occupied orbitals. A careful examination of the MOs for  $\text{C}_5^{2-}$  shows that the four localized pairs of **1** transform as  $a_g + b_{1u} + b_{2u} + b_{3g}$ . Their delocalized equivalents are to be found in  $1b_{2u}$ ,  $b_{eg}$ ,  $2a_g$ , and  $2b_{1u}$  (Figure 7). Two very low-lying MOs ( $a_g$  and  $b_{1u}$ ) with mainly  $s$  character

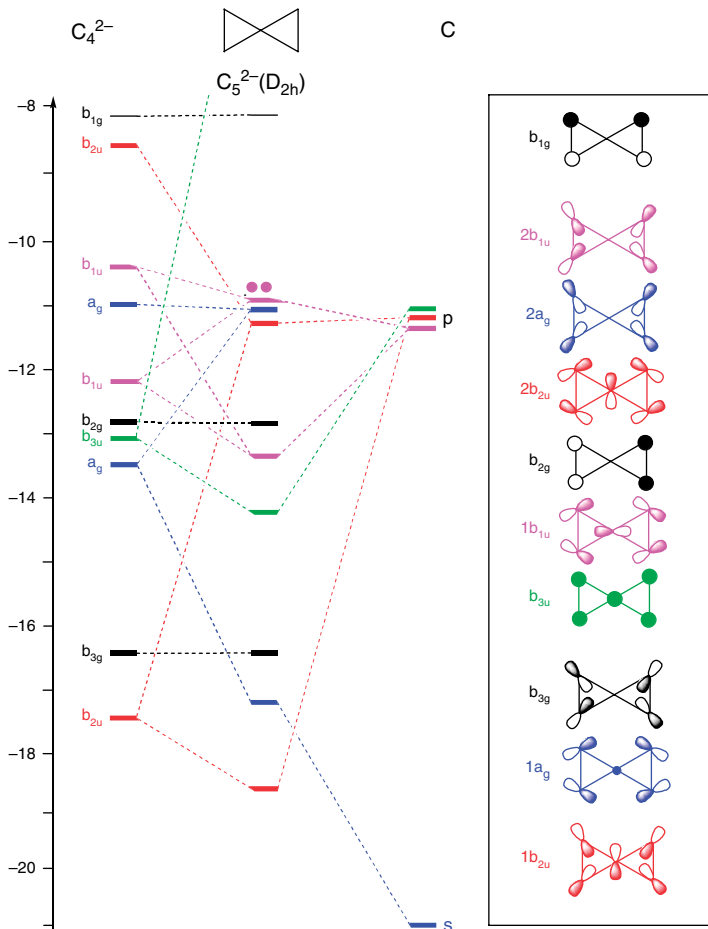


**Figure 7** Correlation diagram between the fragment orbitals of the four “outside” carbon atoms and the central ptC. The bold and thin lines distinguish between filled and empty molecular orbitals

are omitted in the diagram. The destabilization of  $2a_g$  and  $2b_{1u}$  (mostly bonding) over  $1b_{2u}$  and  $b_{3g}$  (mostly antibonding) is due to the interaction with the  $\sigma$  set of MOs. Since these radial MOs mix with the tangential MOs ( $1a_g$ ,  $1b_{1u}$ , and  $2b_{2u}$ ) due to their common symmetry, the orientation of the canonical orbitals differs slightly from those shown schematically in Figure 7. The  $p$ -orbitals perpendicular to the plane, which are involved in the formation of  $\pi$  MOs, are shown as circles, symbolizing their “top” (above the plane) phase. The two  $\pi$  MOs are identified as  $b_{2g}$  and  $b_{2g}$  in Figure 7. The corresponding antibonding combination lies above the LUMO ( $b_{1g}$ ). Note that the  $p$ -orbital of the central carbon atom is the lowest-lying  $p$ -orbital of the carbon framework, covering completely the  $C(C)_4$  skeleton and contributing to the double-bond character of the  $C_2-C'_2$  bond, which turns out to be the fundamental reason to understand the stability of the  $C_5^{2-}$  structure.

It is worth noting that the HOMO and four other occupied MOs of **1** have positive energies, a situation that has been also found in other dianions such as  $\text{CAI}_4^{2-}$  and  $\text{CB}_6^{2-}$ .<sup>43,44</sup> To have any chance of experimentally detecting this structure, it is mandatory to stabilize these orbitals. One possibility is to introduce positive charges into the parent dianion. This idea was used to detect  $\text{CAI}_4^{2-}$ , which after “dressing” it with a counter cation, the resulting  $\text{NaCAI}_4^-$  anion was studied by photoelectron spectroscopy. In the present case, we explored the influence of adding several metals ( $\text{Li}^+$ ,  $\text{Na}^+$ ,  $\text{K}^+$ ,  $\text{Cu}^{2+}$ ,  $\text{Be}^{2+}$ ,  $\text{Mg}^{2+}$ ,  $\text{Ca}^{2+}$ , and  $\text{Zn}^{2+}$ ) to the parental structure  $\text{C}_5^{2-}$  (Table 1 and Figure 8). Interestingly, the addition of the cations does not destroy the planarity of the molecules. The bare  $\text{C}_5^{2-}$  anion, **1**, and **3** have  $D_{2h}$  symmetry, while **2** belongs to a  $C_{2v}$  point group. The harmonic analysis of these molecular structures reveals that they are local minima. As it can be seen in Table 1, adding one counterion with a formal charge of +1 ( $\text{M} = \text{Li}, \text{Na}, \text{K}$ , and  $\text{Cu}$ ) does not change the planarity of

**Table 1** Selected bond lengths (in picometers), angles (in degrees), and smallest frequencies, Freq (in  $\text{cm}^{-1}$ ) of **1–3**.

M	n	C <sub>1</sub> -C <sub>2</sub>	C <sub>1</sub> -C' <sub>2</sub>	C <sub>2</sub> -C' <sub>2</sub>	C' <sub>2</sub> -M	C <sub>2</sub> -C <sub>1</sub> -C <sub>2</sub>	C <sub>2</sub> -C <sub>1</sub> -C' <sub>2</sub>	Freq	
<b>1</b>	–	2–	150.9	–	133.4	–	127.5	–	168.3
<b>2</b>	Li	1–	151.7	150.6	133.0	193.0	132.4	123.1	218.8
	Na	1–	152.5	148.7	132.8	230.5	130.7	124.7	157.4
	K	1–	152.6	149.0	132.8	261.4	128.2	127.3	120.0
	Cu	1–	150.8	150.3	133.0	2.002	141.8	113.4	201.5
	Be	0	154.7	149.2	132.8	162.4	141.3	115.1	235.4
	Mg	0	155.3	146.1	132.1	205.3	136.8	119.5	186.9
	Ca	0	154.2	148.2	132.9	225.0	129.6	126.3	174.3
	Zn	0	155.9	144.9	131.6	203.6	142.0	114.6	161.7
<b>3</b>	Li	0	150.1	–	132.8	200.6	127.5	–	172.3
	Na	0	150.0	–	132.7	235.1	127.5	–	81.7
	K	0	150.6	–	132.7	266.8	127.7	–	52.9
	Cu	0	148.9	–	133.4	207.8	126.8	–	85.6
	Be	2	148.5	–	133.3	177.0	126.6	–	195.4
	Mg	2	148.2	–	132.6	215.4	126.9	–	131.4
	Ca	2	149.9	–	132.3	239.7	127.6	–	103.8
	Zn	2	146.1	–	132.5	214.1	126.1	–	65.4

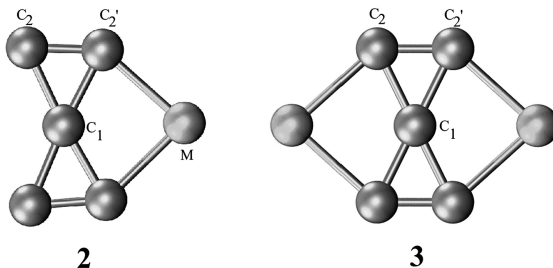


**Figure 8** Schematic representation of **2** and **3**

the structure. The geometrical deformations are more pronounced when one dication is incorporated in the structure. The extreme situation corresponds to C<sub>5</sub>Zn (see Table 1), where the C<sub>1</sub>-C<sub>2</sub> distance increases 5.0 pm and the C<sub>1</sub>-C<sub>2'</sub> distance decreases 6.0 pm. The inclusion of two metal cations produces a reduction of the C<sub>1</sub>-C<sub>2</sub> bond lengths from 0.3(C<sub>5</sub>K<sub>2</sub>) to 4.8 pm(C<sub>5</sub>Zn<sub>2</sub><sup>2+</sup>). Furthermore, the C<sub>2</sub>-C<sub>2'</sub> bond lengths remain practically unchanged after the insertion of one or two metal ions.

In order to gain further insight into the bonding mechanism prevailing in these systems, we perform a topological analysis of the electron density<sup>45</sup> and the electron localization function,<sup>46</sup> as well as a study of their magnetic response to an applied external magnetic field given by the locally induced magnetic field,  $\mathbf{B}^{ind}(\mathbf{r})$ .<sup>47</sup> Any interested reader on this analysis may consult directly our work.<sup>41</sup> From this study, we find that the interaction of the parental C<sub>5</sub><sup>2-</sup> skeleton with the alkaline and alkaline earth atoms is basically ionic, with a remarkable transferability of properties from the isolated dianion to the C<sub>5</sub>M<sub>2</sub> salts. The study of the magnetic response shows that, indeed, the electron delocalization plays a very significant role in stabilizing these ptC-containing compounds.

All the theoretical evidence indicate that C<sub>5</sub>Li<sub>2</sub> is a good candidate for experimental isolation. This molecule has several interesting properties: it is planar, like the parent C<sub>5</sub><sup>2-</sup> anion, it is the hardest, and one of the most diatropic. However, the experimental observation of C<sub>5</sub>Li<sub>2</sub> also depends on the possible rearrangements to more stable isomers. For C<sub>5</sub><sup>2-</sup>, the rearrangement barrier is only 12.6 kJ mol<sup>-1</sup>, including the zero-point energy correction, but the inclusion of two lithium cations increases this barrier to 58.3 kJ mol<sup>-1</sup> (Figure 9). Furthermore, the energy difference between the planar structure of C<sub>5</sub><sup>2-</sup> and the closest isomer is -184.0 kJ mol<sup>-1</sup>, while for C<sub>5</sub>Li<sub>2</sub>, this value is appreciably smaller (-17.4 kJ mol<sup>-1</sup>). Therefore, the isomerization barrier in C<sub>5</sub>Li<sub>2</sub> is sufficiently high to support our optimism that this molecule can be experimentally detected.

Is it possible to build C<sub>5</sub>Li<sub>2</sub> polymers? The design of a fragment containing two C<sub>5</sub><sup>2-</sup> units (a dimer) would require including four monocations keeping the electroneutrality of the system. The relative stabilities of the monomers give an idea on how one can arrange the metal ions around the C<sub>5</sub> unit (Figure 10). The most stable isomer in the C<sub>5</sub>Li<sub>2</sub> series was **4**, suggesting two alternative arrangements for a C<sub>10</sub>Li<sub>3</sub><sup>-</sup> dimer, one where both C<sub>5</sub><sup>2-</sup> units are coplanar, **5**, and another, where the units are perpendicular to each other, **7** (Figure 10). Structure **7** is a minimum on the PES, while **5** has two imaginary frequencies. In the optimized structure of C<sub>10</sub>Li<sub>4</sub>, **6**, two of the Li<sup>+</sup> ions occupy positions between the terminal carbons which are not linked to each other. To gain further insight into the preferred position of the metal, a trimer C<sub>15</sub>Li<sub>6</sub><sup>2-</sup>, **8**, was

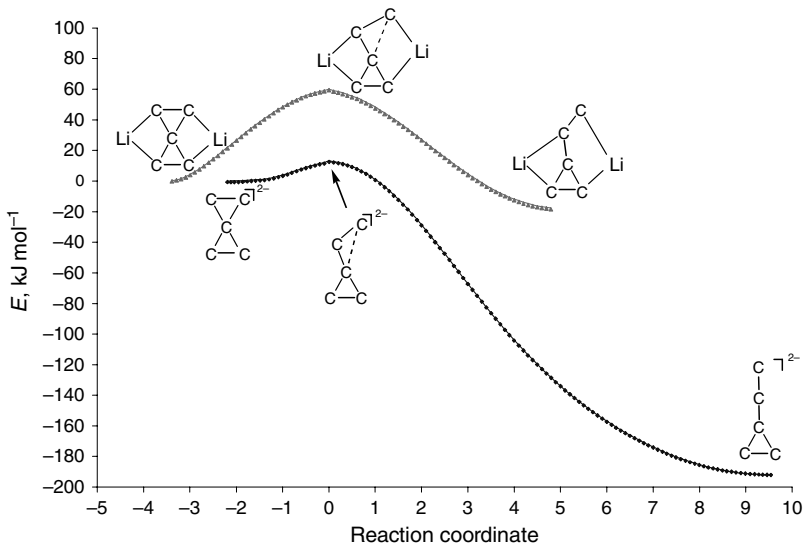


**Figure 9** Energy profiles for the isomerization of  $\text{C}_5^{2-}$  and  $\text{C}_5\text{Li}_2$ . The origin of both reaction paths is the corresponding transition state

also constructed. Both **7** and **8** are minima and continue the bonding motif found for  $\text{C}_5\text{Li}_4^{2+}$ , **9**. These results provided clues for designing extended systems in 2D and 3D containing a ptC.

## 2.2. *ptCs in extended systems*<sup>48</sup>

The idea of having an extended network based on structures containing a ptC, surrounded by diverse elements, has been explored in the past by several authors (Figure 11). One of the first works in this field was again from the mind behind the idea of ptCs. Merschrod, Tang, and Hoffmann built an unusual nickel carbide network,  $[\text{Ni}_3\text{C}_5]^{2-}$ , with repetitive units  $(\text{CNi}_4)^{4-}$ , featuring infinite 1D vertex-sharing chains on Ni squares. Each square was centered by a carbon and flanked by  $\text{C}_2$  units. The orbital interaction schemes revealed that there is little Ni-Ni bonding and essentially no Ni to  $\text{C}_2$  back-donation. However, in this case, the tetrahedral alternative is favored over the planar building block.<sup>49</sup> Later, Li *et al.* discussed the possibility of designing new materials containing pentaatomic ptC species as building blocks for bulk solid materials, based on  $\text{CAI}_4^{2-}$ . Their findings pointed out that bulk solid materials with the composition  $(\text{M}^+)_2[\text{CAI}_4^{2-}]$  may be prepared.<sup>26</sup> Geske and Boldyrev performed *ab initio* calculations on the  $(\text{Na}_2[\text{CAI}_4])_2$  dimer in order to test if the two  $\text{CAI}_4^{2-}$  groups react to form a more stable dimeric structure, or if the two  $\text{CAI}_4^{2-}$  groups remain separated in a true dimeric structure. They established that structures with the C-C bond are higher in energy than the structures with two isolated structural  $\text{CAI}_4^-$  units separated by more than 5 Å, with their structural and electronic integrity preserved. However, alternative structures involving reaction between two  $\text{CAI}_4^{2-}$  groups forming a  $\text{C}_2\text{Al}_8^{4-}$  cluster without the C-C bond are higher in energy, but they are still competitive with the true dimeric structure.

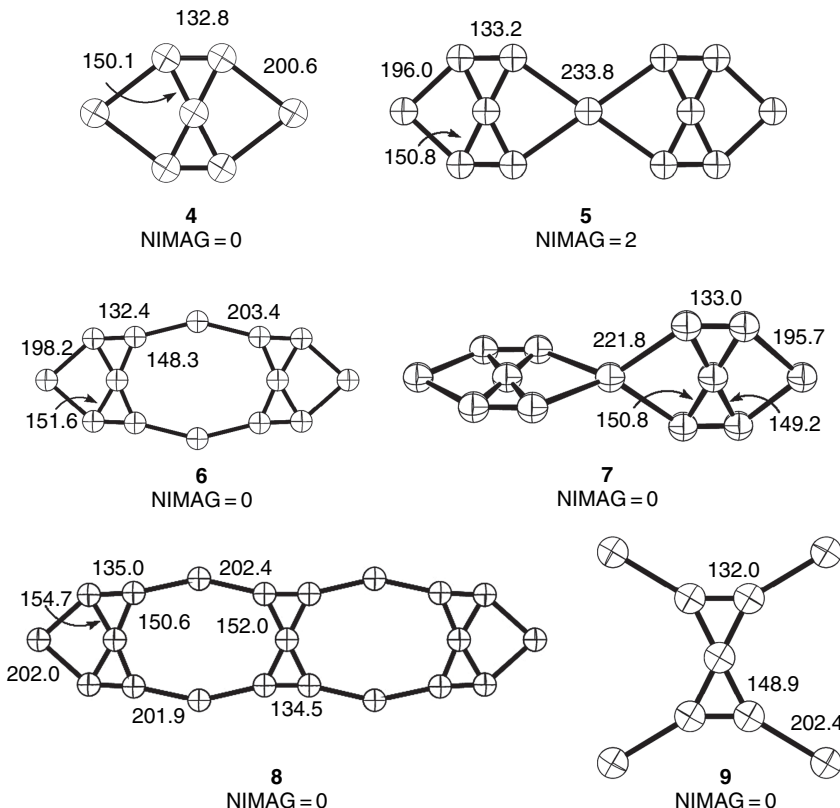


**Figure 10** Optimized structures of  $\text{C}_5\text{Li}_2$ ,  $\text{C}_{10}\text{Li}_3^-$ ,  $\text{C}_{10}\text{Li}_4$ , and  $\text{C}_{15}\text{Li}_6^{2-}$

While they found alternative structures of  $\text{Na}_4\text{C}_2\text{Al}_8$  with the energy comparable to that of the true dimer, they claimed that a solid ionic salt with the pentaatomic tetracoordinate planar carbon  $[\text{CAL}_4]^{2-}$  building block may have good chances to be synthesized, making it the first solid containing a pentaatomic ptC.<sup>50</sup> None of these attempts were successful enough to stabilize a ptC surrounded only by carbon atoms.

Based on our previous calculations on the stability of dimeric and trimeric structures, different 1D and 2D networks were built. The stable dimers **6** and **7**, as well as structure **5**, lend themselves to extension to 1D chains of  $\text{C}_5$  units. These polymeric chains are depicted in Figure 12 as **I**, **II**, and **III**. Since the ratio of a  $\text{C}_5$  unit to the metal in a unit cell of **I** and **III** is 1:1, a divalent metal ion is needed to compensate for the  $-2$  charge on  $\text{C}_5$ . In the case of **II**, the 1:2  $\text{C}_5$  to metal ratio requires a singly charged cation like  $\text{Li}^+$ . If  $\text{Li}^+$  is replaced by a divalent tetracoordinate metal ion, **II** can be converted into a 2D network **IV**, as shown in Figure 12.

Structure **I** requires a tetrahedral coordination around the metal and a divalent metal ion ( $\text{Zn}^{2+}$  or  $\text{Be}^{2+}$ , for example, as these ions have been found before in similar systems such as  $[\text{Zn}(\text{CN})_2]_n$  and  $[\text{CBe}_2]_n$ ). Structure **II** may use  $\text{Li}^+$  ions, meanwhile  $\text{Pt}^{2+}$  may be the right choice for structures **III** and **IV**, as it often exists in a square planar arrangement. In fact, the theoretical analysis showed that compounds **I-Zn**<sup>2+</sup> and **II-Li**<sup>+</sup> were stable, having a tetragonal and orthorhombic unit cells, respectively (Figure 13),

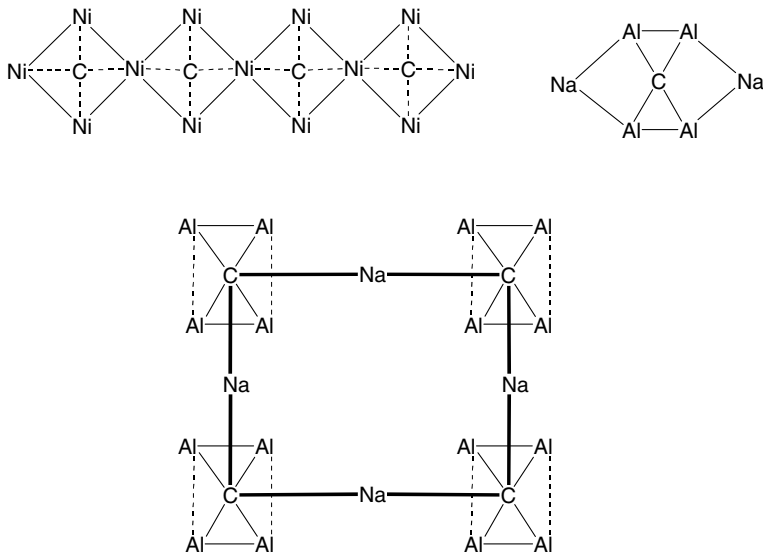


**Figure 11** Several extended network based on structures containing a ptC

but not **I**-Be<sup>2+</sup>, which even failed to converge. The optimized lattice parameters of the different [C<sub>5</sub>M<sub>x</sub>]<sub>n</sub> systems studied are given in Table 2.

Calculations of the band structure and total density of states (DOS) for [C<sub>5</sub>Zn]<sub>n</sub> and [C<sub>5</sub>Li<sub>2</sub>]<sub>n</sub> show large band gaps, suggesting that these solids have semiconducting or insulating behavior. The same situation happens for all other extended network systems. For [C<sub>5</sub>Pt]<sub>n</sub>, it was found that **III** in Figure 14 was preferred over **IV**, which agrees with the relative stabilities of the isomeric forms of C<sub>5</sub>Li<sub>4</sub><sup>2+</sup>.

Thus, this study shows that C<sub>5</sub><sup>2-</sup> is a building block that generates interesting crystal structures having ptCs and semiconducting isolating properties.

### 2.3. ptCs in cyclic hydrocarbons<sup>51</sup>

As the electronic strategy to stabilize a ptC derived from the C<sub>5</sub><sup>2-</sup> unit was shown to be successful, the next logic step was to start building around this unit a hydrocarbon skeleton that could enhance its stability. The main goal in this point is to avoid the isomerization process which is energetically favored toward finding linear carbon chains. Very recently, we started to explore a series of cyclic hydrocarbons containing a ptC(C)<sub>4</sub>.<sup>51</sup> Candidates were obtained by combining the parental C<sub>5</sub><sup>2-</sup> anion with an unsaturated fragment: two hydrogens from ethane and 1,3-dibutadiene were removed, providing the corresponding dications which interact with C<sub>5</sub><sup>2-</sup>, yielding the five- and seven-membered ring systems C<sub>7</sub>H<sub>2</sub>, **10**, and C<sub>9</sub>H<sub>4</sub>, **12**, respectively. The same strategy was used to build the six- and eight-membered anionic rings C<sub>8</sub>H<sub>3</sub><sup>-</sup>, **11**, and C<sub>10</sub>H<sub>5</sub><sup>-</sup>, **13**, from allyl and pentadienyl anions. Their structures are depicted in Figure 15. The harmonic analysis shows that all of them are local minima on their respective PES with an appreciable positive lowest vibrational frequencies (>100 cm<sup>-1</sup>).

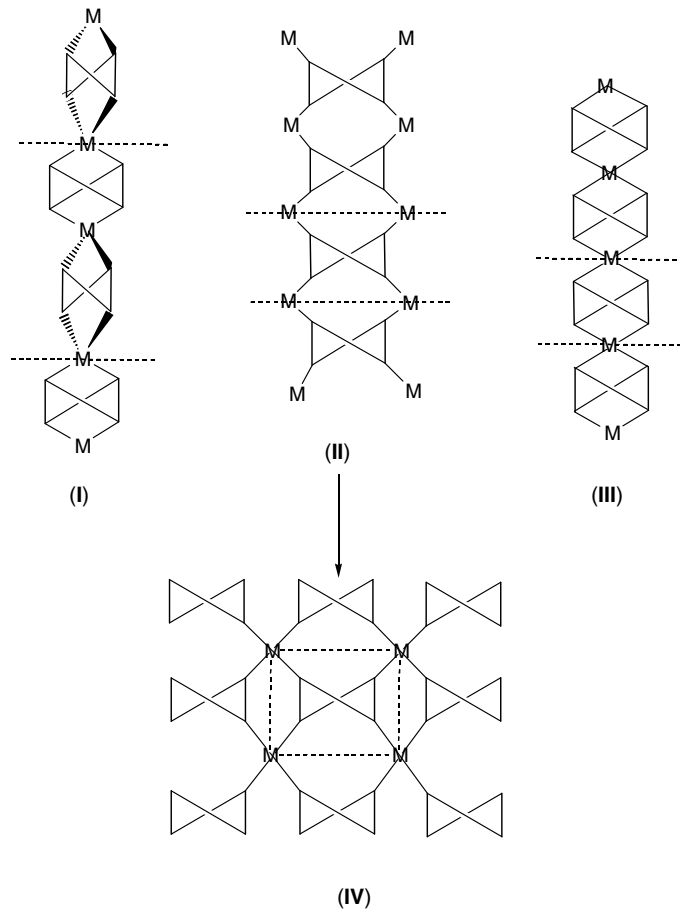


**Figure 12** A schematic diagram for a 1D (**I**, **II**, **III**) and a 2D (**IV**) pattern of  $C_5^{2-}$  units bridged by appropriate metal ions. The repeating units are shown by dashed lines

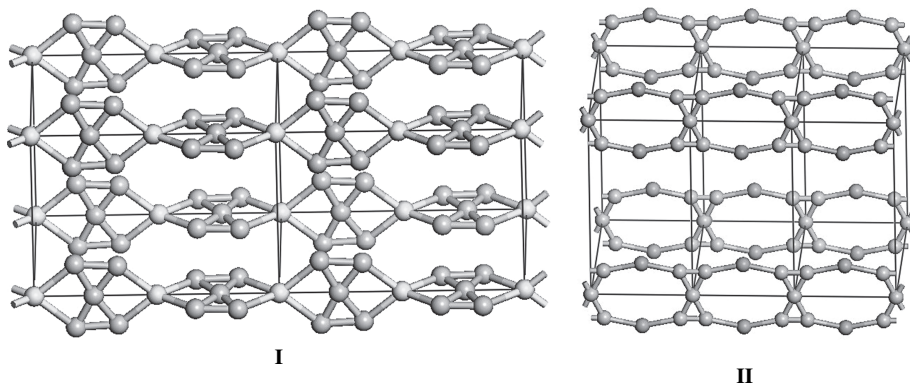


**Figure 13** Optimized lattice of (**I**)  $C_5Zn$  and (**II**)  $C_5Li_2$

**Table 2** Cell parameters ( $a$ ,  $b$ ,  $c$  in Å) and  $V$  (volume in Å $^3$ ) of the different  $C_5M_x$  systems are given

System	$a$	$b$	$c$	$V$
$C_5Zn(I)$	9.90	9.90	9.33	915.14
$C_5Li_2$	5.33	9.91	9.97	526.80
$C_5Pt$	3.84	4.46	5.22	89.32
$C_5Zn(V)$	4.76	4.76	9.14	206.56
$C_5Be$	4.45	4.45	8.82	174.83
$C_5Zn(VII)$	3.78	3.78	10.53	150.46
$C_5Ni$	3.82	3.82	10.44	152.04

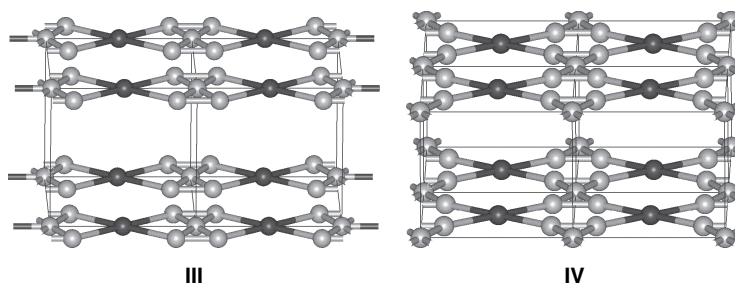


**Figure 14** The 3D unit cells of the **III** and **IV** forms of  $C_5Pt$  are shown

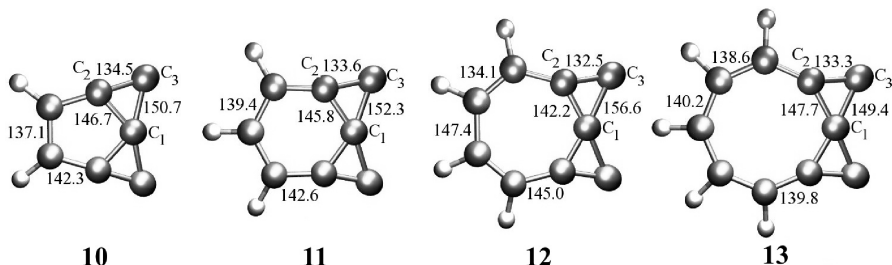


**Figure 15** Optimized structures of cyclic hydrocarbons containing a ptC. Bond lengths are given in picometers

As it was mentioned before, the experimental detection of any of these molecules depends on their mean lifetimes. To have an estimate of these lifetimes, a set of Born–Oppenheimer molecular dynamic (BO–MD) trajectories were done. As one can see in Table 3, and as expected, ring-opening is accompanied by a small activation barriers, in the range of 10–40 kJ mol $^{-1}$ . As it can be seen in Figure 16, a typical MD trajectory of **13**, which has the lowest activation barrier, the planar structure preserves its geometry for about 6.0 ps at 300K. This is a very short lifetime but, considering that it corresponds to the hydrocarbon with the smallest activation energy, one can be optimistic that the lifetimes of **10–12** can be large enough for its experimental detection.

**Table 3** Smallest frequencies (Freq) in  $\text{cm}^{-1}$ , energy difference between the ptC molecule and its closest isomer ( $\Delta E$ ), and its corresponding activation energy,  $E_a$ .

	<b>10</b>	<b>11</b>	<b>12</b>	<b>13</b>
Freq	246.3	169.0	102.0	150.1
$\Delta E$	-42.4	-28.9	-52.1	-110.7
$E_a$	38.0	23.1	30.7	10.7

All energies are in  $\text{kJ mol}^{-1}$ .

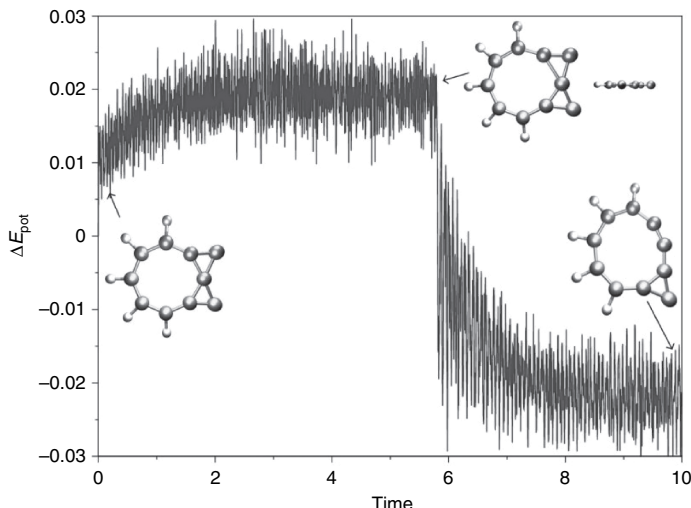


**Figure 16** BO–MD simulation of molecule **13**. Relative potential energy ( $\Delta E_{\text{pot}}$ ) (in a.u.) vs. time (in ps)

The MOs of these molecules that contribute more to their stability are shown in Figure 17. Clearly, the lowest-lying  $\pi$ -orbitals ( $b_1$  symmetry) have an important contribution from the central  $\pi$ -type lone pair, and it is essentially distributed over the entire  $\text{C}(\text{C})_4$  skeleton. The HOMOs of the neutral species **10** and **12** are in-plane lone pairs of the carbon atoms labeled as  $C_3$ . In contrast, in the anions **11** and **13**, the HOMOs are  $\pi$ -orbitals. The number of  $\pi$  electrons in each molecule is six in **10**, eight in **11** and **12**, and ten in **13**. It should be noted that cyclic hydrocarbons containing  $(4n+2)\pi$  electrons (**10** and **13**) preserve the  $\text{C}_5^{2-}$  fragment almost intact.

We have also explored the electron delocalization and magnetic response of these molecules. All have strong diatropic contributions inside the three-membered rings that constitute the  $\text{C}_5$  skeleton. For the  $(4n+2)\pi$ -electron species (**10** and **13**), the main cycles of the molecules have an aromatic response, while for the  $8\pi$ -electron cycles (**11** and **12**), they show an antiaromatic response. Isosurfaces of the  $z$ -component of  $\mathbf{B}^{\text{ind}}(\mathbf{B}^{\text{ind}}_z)$  of the molecules are shown in Figure 18. The aromatic molecules have a strongly shielding region close to the carbons inside the ring, which resembles the form

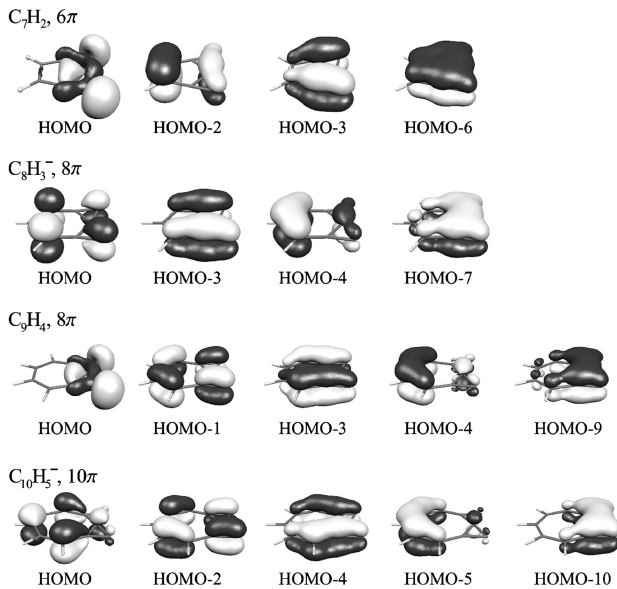


**Figure 17** HOMOs and  $\pi$ -MOs ( $|\varphi| = 0.05$  a.u.) for **10–13**

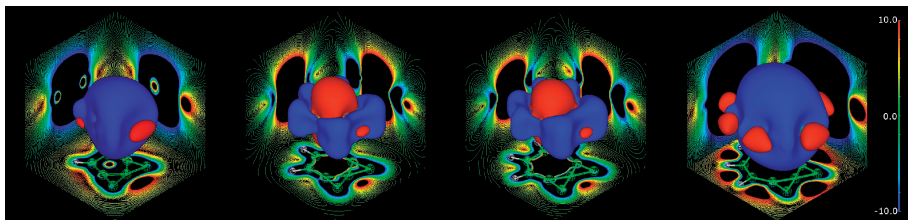


**Figure 18** Isosurfaces of the  $z$ -component of the induced magnetic field,  $\mathbf{B}^{ind}_z$ .  $|\mathbf{B}^{ind}_z| = 9.0 \mu\text{T}$  and  $|\mathbf{B}^{ext}| = 1.0 \text{ T}$ , perpendicular to the molecular plane. Blue and red indicate shielding ( $|\mathbf{B}^{ind}_z| < 0$ ) and deshielding areas, respectively

of the carbon  $\pi$ -orbitals. The antiaromatic molecules show a deshielding cone *outside* the ring, with the carbon atoms just inside the deshielding region.

We are currently exploring the electronic, magnetic, and structural characteristics of several new members of this cyclic hydrocarbon family. Symmetric and asymmetric systems, with rings of different size at each side, are showing an increased stability due to the size and symmetry of these hydrocarbons.

### 3. Future perspectives on ptCs derived from $\text{C}_5^{2-}$ (and its experimental detection)

The most important messages that we have learned from our studies about ptC-containing molecules are that the delocalization of the lone pair located in the central carbon atom and the size of the energy barriers that prevent the isomerization of the molecule

are among the most important factors to be considered in the molecular engineering of these species. Taking into account these crucial factors, we are presently studying systems where these rearrangements are decreased, or even better, stopped completely. By learning these theoretical “know-hows”, we are optimistic that we will see *in vitro*, and in our lifetimes, the experimental detection of some of these *in silico* designed molecules that challenge one of the paradigms of organic chemistry.

## Acknowledgments

We are grateful to many colleagues for their collaboration in this project: Thomas Heine, Gotthard Seifert, and Robert Barthel (Technische Universität Dresden), Pattath D. Pancharatna (Cornell University), Clemence Corminboueuf (University of Geneva), Hiram I. Beltrán (Instituto Mexicano del Petróleo), and Nancy Perez (Universidad de las Américas). We owe special thanks to Prof. Roald Hoffmann for his thorough and thoughtful inspiration of this work. We gratefully acknowledge the support from CONACYT (Projects G34037-E and G32710-E), Deutsche Forschungsgemeinschaft (DFG), and Decanatura de Investigación y Posgrado (DIP-UDLA).

## References

1. Frankland, E., *Phil. Trans. Roy. Soc.* **1852**, 142, 417.
2. Couper, A. S., *Ann. Chem.* **1859**, 110, 46.
3. Kekule, A., *Bull. Soc. Chim. Fr.* **1965**, 3, 98.
4. van't Hoff, J. H., *Arch. Neerl. Sci. Exactes Nat.* **1874**, 445.
5. LeBel, J. A., *Bull. Soc. Chim. Fr.* **1874**, 22.
6. Tal'roze, V. L.; Lyubimova, A. K., *J. Mass Spectr.* **1998**, 33, 502.
7. <http://nobelprize.org/chemistry/laureates/1994/>.
8. Hoffmann, R.; Alder, R. W.; Wilcox, C. F., *J. Am. Chem. Soc.* **1970**, 92, 4992.
9. Siebert, W.; Gunale, A., *Chem. Soc. Rev.* **1999**, 28, 367.
10. Erker, G., *Chem. Soc. Rev.* **1999**, 28, 307.
11. Collins, J. B.; Dill, J. D.; Jemmis, E. D.; Apeloig, Y.; Schleyer, P. v. R.; Seeger, R.; Pople, J. A., *J. Am. Chem. Soc.* **1976**, 98, 5419.
12. Erker, G.; Rottger, D., *Angew. Chem. Int. Edit. Engl.* **1993**, 32, 1623.
13. Radom, L.; Rasmussen, D. R., *Pure Appl. Chem.* **1998**, 70, 1977.
14. Sorger, K.; Schleyer, P. v. R., *Theochem-J. Mol. Struct.* **1995**, 338, 317.
15. Priyakumar, U. D.; Reddy, A. S.; Sastry, G. N., *Tetrahedron Lett.* **2004**, 45, 2495.
16. Priyakumar, U. D.; Sastry, G. N., *Tetrahedron Lett.* **2004**, 45, 1515.
17. Li, S.-D.; Ren, G.-M.; Miao, C.-Q.; Jin, Z.-H., *Angew. Chem. Int. Edit.* **2004**, 43, 1371.
18. Sahin, Y.; Prasang, C.; Hofmann, M.; Subramanian, G.; Geiseler, G.; Massa, W.; Berndt, A., *Angew. Chem. Int. Edit.* **2003**, 42, 671.
19. Minyaev, R. M.; Minkin, V. I.; Gribanova, T. N.; Starikov, A. G.; Hoffmann, R., *J. Org. Chem.* **2003**, 68, 8588.
20. Huang, J. H.; Luci, J. J.; Lee, T. Y.; Swenson, D. C.; Jensen, J. H.; Messerle, L., *J. Am. Chem. Soc.* **2003**, 125, 1688.
21. Minkin, V. I.; Minyaev, R. M.; Hoffmann, R., *Uspekhi Khimii* **2002**, 71, 989.
22. Schleyer, P. v. R.; Boldyrev, A. I., *J. Chem. Soc. Chem. Commun.* **1991**, 1536.
23. Boldyrev, A. I.; Simons, J., *J. Am. Chem. Soc.* **1998**, 120, 7967.

24. Li, X.; Wang, L. S.; Boldyrev, A. I.; Simons, J., *J. Am. Chem. Soc.* **1999**, 121, 6033.
25. Boldyrev, A. I.; Li, X.; Wang, L. S., *Angew. Chem. Int. Edit.* **2000**, 39, 3307.
26. Li, X.; Zhang, H. F.; Wang, L. S.; Geske, G. D.; Boldyrev, A. I., *Angew. Chem. Int. Edit.* **2000**, 39, 3630.
27. Wang, L. S.; Boldyrev, A. I.; Li, X.; Simons, J., *J. Am. Chem. Soc.* **2000**, 122, 7681.
28. Boldyrev, A. I.; Wang, L. S., *J. Phys. Chem. A* **2001**, 105, 10759.
29. McGrath, M. P.; Radom, L., *J. Am. Chem. Soc.* **1993**, 115, 3320.
30. Rasmussen, D. R.; Radom, L., *Angew. Chem. Int. Edit.* **1999**, 38, 2876.
31. Dodziuk, H., *J. Mol. Struct.* **1990**, 239, 167.
32. Dodziuk, H.; Leszczynski, J.; Nowinski, K. S., *J. Org. Chem.* **1995**, 60, 6860.
33. Dodziuk, H.; Leszczynski, J.; Nowinski, K. S., *Theochem-J. Mol. Struct.* **1997**, 391, 201.
34. Dodziuk, H.; Nowinski, K. S., *Theochem-J. Mol. Struct.* **1994**, 117, 97.
35. Thommen, M.; Keese, R., *Synlett* **1997**, 231.
36. Wang, Z. X.; Schleyer, P. v. R., *J. Am. Chem. Soc.* **2001**, 123, 994.
37. Wang, Z. X.; Schleyer, P. v. R., *J. Am. Chem. Soc.* **2002**, 124, 11979.
38. Merino, G.; Mendez-Rojas, M. A.; Vela, A., *J. Am. Chem. Soc.* **2003**, 125, 6026.
39. Bernath, P. F.; Hinkle, K. H.; Keady, J. J., *Science* **1989**, 244, 562.
40. Dua, S.; Bowie, J. H., *J. Phys. Chem. A* **2002**, 106, 1374.
41. Merino, G.; Mendez-Rojas, M. A.; Beltran, H. I.; Corminboeuf, C.; Heine, T.; Vela, A., *J. Am. Chem. Soc.* **2004**, 126, 16160.
42. Rao, V. B.; George, C. F.; Wolff, S.; Agosta, W. C., *J. Am. Chem. Soc.* **1985**, 107, 5732.
43. Li, X.; Zhai, H. J.; Wang, L. S., *Chem. Phys. Lett.* **2002**, 357, 415.
44. Exner, K.; Schleyer, P. v. R., *Science* **2000**, 290, 1937.
45. Bader, R. F. W., *Atoms in Molecules. A Quantum Theory*. ed.; Oxford University Press: Oxford, 1990.
46. Silvi, B.; Savin, A., *Nature* **1994**, 371, 683.
47. Merino, G.; Heine, T.; Seifert, G., *Chem. Eur. J.* **2004**, 10, 4367.
48. Pancharatna, P. D.; Mendez-Rojas, M. A.; Merino, G.; Vela, A.; Hoffmann, R., *J. Am. Chem. Soc.* **2004**, 126, 15309.
49. Merschrod, E. F.; Tang, S. H.; Hoffmann, R., *Z. Naturforsch. B* **1998**, 53, 322.
50. Geske, G. D.; Boldyrev, A. I., *Inorg. Chem.* **2002**, 41, 2795.
51. Perez, N.; Heine, T.; Barthel, R.; Seifert, G.; Vela, A.; Mendez-Rojas, M. A.; Merino, G., *Org. Lett.* **2005**, 7, 1509.